MODELLING OF LOW FREQUENCY LONGITUDINAL COUPLED BUNCH OSCILLATION

R. Nagaoka* and A. Wrulich
Sincrotrone Trieste, Padriciano 99, 34012 Trieste, Italy

Abstract

The paper describes development of a theoretical model to interpret the observed low frequency beam oscillation in ELETTRA and compares the calculated results with the measurements.

1. INTRODUCTION

A notable beam instability observed in ELETTRA since the early times is one which associates a Low Frequency Oscillation referred to as LFO, in the frequency range below 100 Hz, which can be observed on the signals from a stripline or a capacitive button electrode with a low frequency spectrum analyser. LFOs were observed particularly at low beam current typically below 100 mA, where the frequency was noticed to increase quasi linearly with beam current. As the correlation had been verified in detail with the Higher Order Modes (HOMs) of the cavities which can be tuned with the cavity temperatures[1], it became clear that the LFO is triggered by a Longitudinal Multi Bunch Instability (LMBI)[2]. A question however remained to be understood how a LMBI could cause LFOs. The first clue was given by pursuing the energy dependence, which suggested radiation damping to be involved as the frequency in many cases increases with energy roughly as E^3.

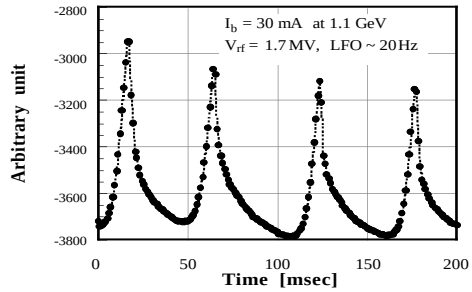

Fig. 1. Observed signal on a capacitive electrode.

A more definitive evidence was then given by performing a BPM digitalisation where a button electrode, triggered by the RF, continuously acquires the induced voltage at every one millisecond (Fig. 1). The induced voltage, which should represent the average longitudinal displacement of a beam with respect to the synchronous position, shows a fast rise followed by a slower decay whose rate is close to the longitudinal damping. Another decisive observation was the time variation of the amplitude of the synchrotron frequency, measured with the tune measurement pickups. Compared to the former, the amplitude which emerges synchronously with the LFO decays much faster in time.

These observations lead us to interpret the LFOs to be a coherent synchrotron motion excited by LMBIs growing rapidly until the amplitude reaches a nonlinear region where the motion is Landau damped. The blown up beam will then be subject to radiation damping until it recovers the coherence again. In the literature, we find similar observations to exist in other machines as well [3,4]. In Ref. 3, in particular, where detailed measurements and analysis are made, the author describes it as a coherent synchrotron relaxation oscillation.

Since all ingredients which appear in the model derived above are basically known, we shall attempt to develop further the model quantitatively to justify the picture itself, and then to seek for the reproducibility of the observations, also trying to understand what are the essential features.

2. THE DEVELOPED MODEL

As the difference in time scale of individual processes is expected to be critically important in understanding the evolution of a system which particularly is supposed to involve a loss of coherence, it appears suitable to perform a multi particle tracking to study the system. We therefore develop a longitudinal tracking which includes the effects of the nonlinear RF field, radiation damping and a collective wake force. A quantity of interest is the phase space amplitude averaged over the particles, $F \equiv \langle x^2 + (\alpha_c/\omega_s \cdot \varepsilon)^2 \rangle^{1/2}$, which would correspond to the voltage seen by the BPM. Here, (x, ε) denote time and energy coordinates, α_c the momentum compaction, and ω_s is the angular synchrotron frequency.

Instead of treating the wake force rigorously in terms of a wake function and a time dependent distribution, we take for simplicity a semi phenomenological approach to include this effect in parallel with radiation damping via grow rate $1/\tau_u$ calculated from the formulae. The relation assumed in the tracking of a single particle thus reads

$$\varepsilon_{new} = \varepsilon_{old} + \frac{V_{rf}}{E_0} \cdot [\sin(\omega_{rf} x_{old} + \phi_0) - \sin\phi_0] - D_e \cdot \varepsilon_{old} + D_u \cdot \varepsilon_{CM}, \quad (1)$$

$$x_{new} = x_{old} + T_0 \alpha_c \cdot \varepsilon_{new}, \quad (2)$$

where the meaning of symbols are as follows;

V_{rf}: RF voltage, ω_{rf}: Angular RF frequency,
ϕ_0: Synchronous angle, E_0: Beam energy,
T_0: Revolution period.

*Present address: ESRF, BP220, 38043 Grenoble Cedex, France, which supports the presentation of this work.

D_e is related to radiation damping rate $1/\tau_e$ by $D_e = 2(1/\tau_e)T_0$, and D_u likewise to $1/\tau_u$. It is noted that, reflecting a mean field, the term with D_u is multiplied by the centre of mass coordinate ε_{CM}. The effect of potential well distortion as well as coherent tune shift are regarded irrelevant and not considered. In most cases, 500 particles were tracked over 200 msec, which requires nearly 10 minutes of cpu time. Results are confirmed to depend little on the number of particles.

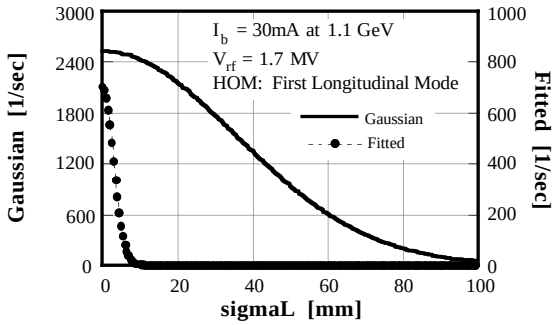

Fig. 2. Growth rate $1/\tau_u$ versus longitudinal beam size σ_L.

We initiated our study from using $1/\tau_u$ calculated from the standard formula derived for a Gaussian beam, with impedance values of the first longitudinal mode which is identified to excite the LFOs (Fig. 2) [1]; Shunt impedance R = 1600 kΩ, quality factor Q = 45000 and the beam harmonic = 821. Tracking was performed starting from the nominal Gaussian beam. We basically find that the assumed growth rate, with the nonlinearity of the ordinary RF field, does lead to a loss of coherence, namely to a filamentation, around an amplitude in phase space which is in a reasonable range as compared to the measurements. However, after the initial blow up, the system only reaches an equilibrium, as typically shown in Fig. 3. Note that the beam size σ_L is evaluated at each instant with

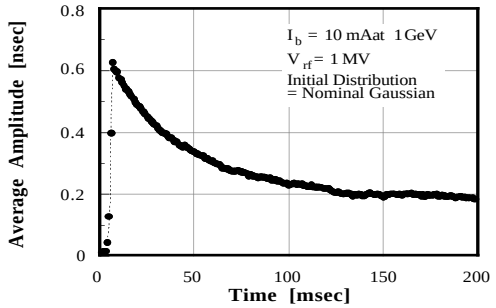

Fig. 3. Average amplitude F obtained from the tracking with $1/\tau_u$ calculated assuming a Gaussian distribution.

which $1/\tau_u$ is computed. The result signifies that the reduction in the wake force due to lowering of the growth rate $1/\tau_u$ for larger σ_L (cf. Fig. 2), together with decreasing magnitude of ε_{CM} due to the loss of coherence, are not adequate to explain the saw tooth mechanism (see Eq. 1).

In fact, the observations (Fig. 1) indicate that after the filamentation, the beam is subject to damping over a major part of an oscillation period, which implies that the wake force during this interval is actually vanishing. In terms of growth rate, this means that its decay as a function of σ_L, the "effective" beam size of a filamented beam, should be much faster than what is given by the Gaussian formula, suggesting that $1/\tau_u$ needs to be re-evaluated for the completely different beam distribution.

Here we refer to the work of Ref. 5 where analytical expressions for the complex coherent frequency shifts are derived by solving the Sacherer's equation for extreme beam models; a water bag, in the longitudinal, and a hollow bunch in the transverse motions. The multi-turn sums are in particular rigorously evaluated. We apply the developed technique to obtain the growth rate for a hollow bunch in the longitudinal motion. We should stress that the use of a hollow bunch is not for the sake of mathematical simplification, but rather as an approximation of the supposed distribution. Below we merely give the final result for $1/\tau_u$ obtained for the dipole mode. More details will be found elsewhere [6];

$$1/\tau_u = -\pi \sum_{\kappa} \frac{N\alpha_c e^2}{\nu_s T_0^2 E_0} \cdot \frac{\alpha_\kappa R_\kappa}{\omega_{r\kappa}} (1 - a_\kappa^2)$$
$$\times J_1(\rho\omega_{r\kappa}/\omega_0) \cdot [2J_1(\rho\omega_{r\kappa}/\omega_0) - \rho\omega_{r\kappa}/\omega_0 \, J_0(\rho\omega_{r\kappa}/\omega_0)] /\rho^2$$
$$\times \left[\frac{1}{1+a_\kappa^2-2a_\kappa\cos\phi_{1\kappa}} - \frac{1}{1+a_\kappa^2-2a_\kappa\cos\phi_{2\kappa}} \right], \qquad (3)$$

where ρ denotes the radial amplitude of the distribution, κ distinguishes the HOMs, and J_n (n = 0,1) are the Bessel functions. Other symbols signify as follows [5];

N: Number of particles in a bunch,
ω_0: $2\pi/T_0$, ν_s: ω_s/ω_0,
ω_κ: Angular eigenfrequency, α_κ: $\omega_\kappa/2Q_\kappa$,
$\omega_{r\kappa}$: $\omega_\kappa[1 - 1/(4Q_\kappa^2)]^{1/2}$, a_κ: $\exp(-\alpha_\kappa T_0/M)$,
$\phi_{1\kappa}$: $T_0/M\cdot(\omega_{r\kappa} - \omega_s - \mu\omega_0)$, $\phi_{2\kappa}$: $T_0/M\cdot(\omega_{r\kappa} + \omega_s + \mu\omega_0)$,
M: Number of bunches, μ: Coupled bunch number.

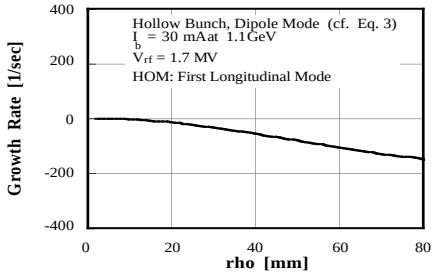

Fig. 4. Growth rate $1/\tau_u$ versus radial amplitude ρ of a hollow bunch (Eq. 3), calculated under same conditions as in Fig. 2.

It turns out that due to the property $2J_1(x) \sim xJ_0(x)$ for $x << 1$, there is a large cancellation in the form factor part of $1/\tau_u$ in Eq. 3, as a result of which, the growth rate is nearly vanishing in the range of interest. It is also noteworthy that $1/\tau_u$ deviates in the negative direction creating a damping effect at larger amplitudes.

3. DISCUSSIONS

As the vanishing of the growth rate $1/\tau_u$ for a filamented beam may be justified as above, we searched empirically for $1/\tau_u$ which would reproduce the observation in Fig. 1, tentatively in the Gaussian form. The optimal $1/\tau_u$ which reproduces the LFO to the extent as shown in Fig. 5a, is compared with that of the Gaussian beam in Fig. 2. The magnitude of the fitted $1/\tau_u$ at origin is considerably smaller and tends to zero before σ_L reaches 10 mm. The effective growth rate on the calculated amplitude in Fig. 5a, however, is in a good agreement with the observation in Fig. 1.

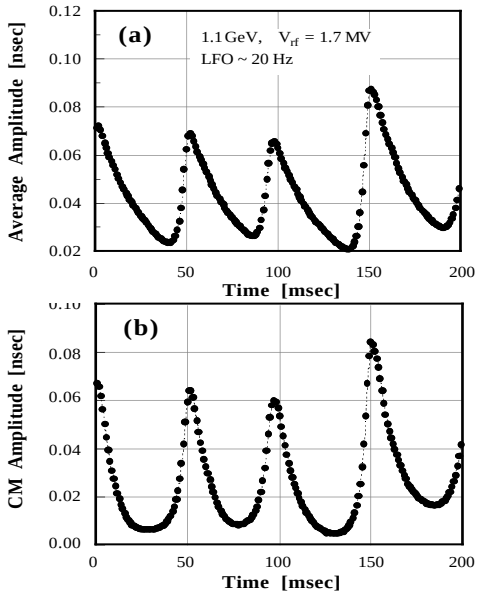

Fig. 5. Calculated (a) average amplitude F, and (b) centre of mass amplitude versus time, obtained with the vanishing $1/\tau_u$ (Fig. 2).

Regarding the measured data, damping tends to be stronger than what expected by typically 50% or even higher for larger amplitudes. The reason is not clear whether it is related to the additional damping effect found above. A better agreement is actually found by increasing the damping rate in the simulation. The shown example in Fig. 5 assumes 50% increase, as well as the additional damping given by Eq. 3 which however is only influential at large amplitudes. The calculated centre of mass amplitude (Fig. 5b) shows expected behaviour which resembles the observed variation of the amplitude of synchrotron frequency in time. The corresponding beam distributions in phase space are shown for several representative instants in Fig. 6. As the filamented beam feels no wake force, it damps sufficiently down to the origin. Once the beam begins to feel the wake force, it oscillates coherently moving its centre outwards until the increasing nonlinearity together with sufficient revolution in phase space brings the beam to be filamented. On the synchrotron radiation profile monitor, two dense spots

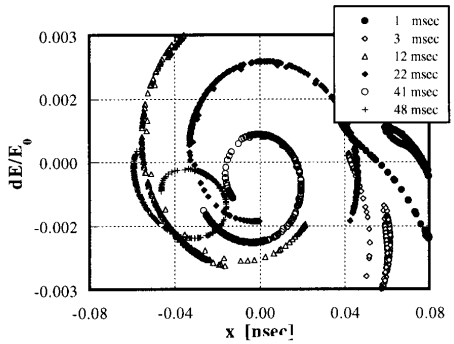

Fig. 6. Calculated phase space beam distributions at various instants in the above tracking (Fig. 5).

may be detected under these circumstances. Thus, it can be said to be the combination of filamentation at large amplitudes and the vanishing of the wake force after filamentation which renders the process irreversible, producing the saw tooth mechanism.

Irregularity of the oscillation is noticed in Figs. 5 where the amplitude grows larger when the preceding damping proceeds to a better degree. Such a trend is observed in reality as well. In fact, as also pointed out in Ref. 3, depending upon a delicate balance among the involved parameters such as cavity temperatures, beam current, energy and the rf voltage, the beam exposes a wide variety of phenomena, including a steady state as shown in Fig. 3. In particular, it may be understood that LFOs are more likely to occur at low energies due to higher growth rate and weaker radiation damping, the latter of which promotes the filamentation. A more detailed analysis on the dependence of the phenomena on different parameters will be found elsewhere [6].

4. ACKNOWLEDGEMENT

The authors are especially grateful to R. De Monte, M. Svandrlik and L. Tosi who took initiatives in many valuable measurements and analysis. They thank C.J. Bocchetta, A. Fabris, F. Iazzourene, E. Karantzoulis, R.P. Walker and all other ELETTRA shift crew for their support on this work.

5. REFERENCES

[1] M. Svandrlik et al., "The Cure of Multibunch Instabilities in ELETTRA", Proc. PAC Dallas (1995).
[2] A. Wrulich et al., "Observation of Multibunch Instabilities in ELETTRA", this conference.
[3] G. Rakowsky, "Coherent Synchrotron Relaxation Oscillation in an Electron Storage Ring", IEEE Trans. Nucl. Sci. **NS-32**, No. 5 (1985) 2377.
[4] Y. Yamazaki et al., "A Longitudinal Coupled-Bunch Oscillation Observed in the KEK-PF Electron Storage Ring", KEK 83-7 (1983) A/P.
[5] T. Suzuki and K. Yokoya, "Simplified Criteria for Bunched Beam Instability due to RF Cavities", Nucl. Instr. Meth. **203** (1982) 45.
[6] R. Nagaoka et al., in preparation.